

Geomorphic observations from southwestern terminus of Palghat Gap, south India and their tectonic implications

YOGENDRA SINGH^{1,2}, BIJU JOHN^{1,2,*}, G P GANAPATHY¹, ABHILASH GEORGE³,
S HARISANTH³, K S DIVYALAKSHMI² and SREEKUMARI KESAVAN⁴

¹*VIT University, Vellore, Tamil Nadu 632 014, India.*

²*National Institute of Rock Mechanics, KGF, Karnataka 563 117, India.*

³*Cochin University of Science and Technology, Kochi, Kerala 682 016, India.*

⁴*National Centre for Earth Science Studies, Thiruvananthapuram, Kerala 695 031, India.*

*Corresponding author. e-mail: b_johnp@yahoo.co.in

The region around Wadakkancheri, Trichur District, Kerala is known for microseismic activity, since 1989. Studies, subsequent to 2nd December 1994 (M=4.3) earthquake, identified a south dipping active fault (Desamangalam Fault) that may have influenced the course of Bharathapuzha River. The ongoing seismicity is concentrated on southeast of Wadakkancheri and the present study concentrated further south of Desamangalam Fault. The present study identifies the northwestern continuity of NW–SE trending Periyar lineament, which appears to have been segmented in the area. To identify the subtle landform modifications induced by ongoing tectonic adjustments, we focused on morphometric analysis. The NW–SE trending lineaments appear to be controlling the sinuosity of smaller rivers in the area, and most of the elongated drainage basins follow the same trend. The anomalies shown in conventional morphometric parameters, used for defining basins, are also closely associated with the NW–SE trending Periyar lineament/s. A number of brittle faults that appear to have been moved are consistent with the present stress regime and these are identified along the NW–SE trending lineaments. The current seismic activities also coincide with the zone of these lineaments as well as at the southeastern end of Periyar lineament. These observations suggest that the NW–SE trending Periyar lineaments/faults may be responding to the present N–S trending compressional stress regime and reflected as the subtle readjustments of the drainage configuration in the area.

1. Introduction

Active fault identification in low-relief, densely populated areas holds special importance as very little work has been done in such areas. However, detection of potential seismic sources in those areas is not an easy task because very few applicable methods exist, especially if the area is characterized by low seismicity. In such areas, morphometric analysis of drainage network is found to be an

appropriate tool (Cox 1994; John and Rajendran 2008). Several studies have documented the influence of vertical crustal movements on the channel pattern, especially in strike-slip tectonic environments (e.g., Ouchi 1985; Jorgensen 1990; Holbrook and Schumm 1999). Following the global trends, there were also some attempts to delineate the signatures of active faulting from drainage anomalies in peninsular India (e.g., Subrahmanya 1996; John and Rajendran 2008; Ramaswamy *et al.* 2011). The

Keywords. Morphometry; river sinuosity; anomalies; brittle faults; earthquakes.

present study is an additional effort to identify signatures of active tectonic elements from an area, which is experiencing mild seismic activity.

The drainage networks in Kerala are considered to be tectonically controlled (Sinha-Roy and Mathai 1979) and majority of the microtremor locations in Kerala show rough parallelism with the drainage courses of some of the major rivers (Rajendran and Rajendran 1996). Our studies are focused in an area where there are reports of microseismic activity since 1989. The studies subsequent to 1994 Wadakkancheri earthquake, identified Desamangalam Fault, which moved in the ongoing compressional stress regime and changed the course of E–W flowing Bharathapuzha River (John and Rajendran 2008).

The present study carried out investigations further south of Desamangalam Fault owing to the occurrence of infrequent seismic activity. It identified the continuity of NW–SE trending Periyar lineament, one of the major faults in Kerala. This lineament appears as subparallel northwest trending segments and has influenced the drainage system.

Southeastern end of this lineament is associated with seismicity (figure 1). This paper presents the observations from geomorphic studies carried out in the northwestern end of the lineament and their relation to brittle faults and sporadic seismicity.

2. Tectonic framework of the area

The study area lies between Bharathapuzha and Chalakkudi rivers and northern half of it is a part of the Proterozoic Palghat–Cauvery Shear Zone (PCSZ) (Bhaskar Rao *et al.* 1996) and is also termed as Palghat Gap, a conspicuous geomorphic break. The west-flowing Bharathapuzha River, traverses through the central part of the 30 km wide gap area. The E–W trending structural elements in the gap region (PCSZ) may have been associated with Proterozoic tectonic events defined by a large E–W dextral oblique-slip component (D’Cruz *et al.* 2000) and is mainly confined to the northern side of Bharathapuzha River (figure 2). However, the area south of the main trunk of the

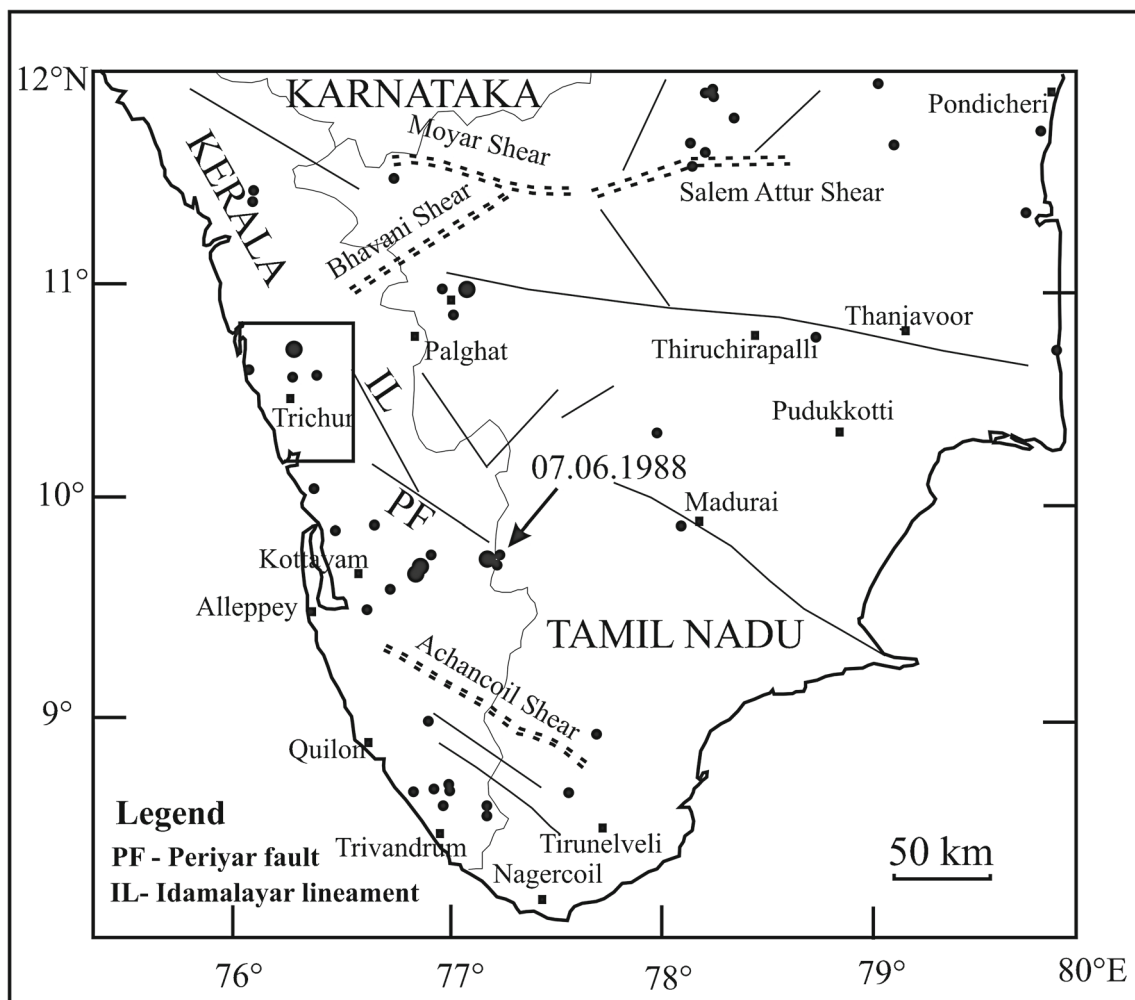


Figure 1. Seismotectonic map of south India adopted from SEISAT (GSI 2000). The study area is shown in rectangle.

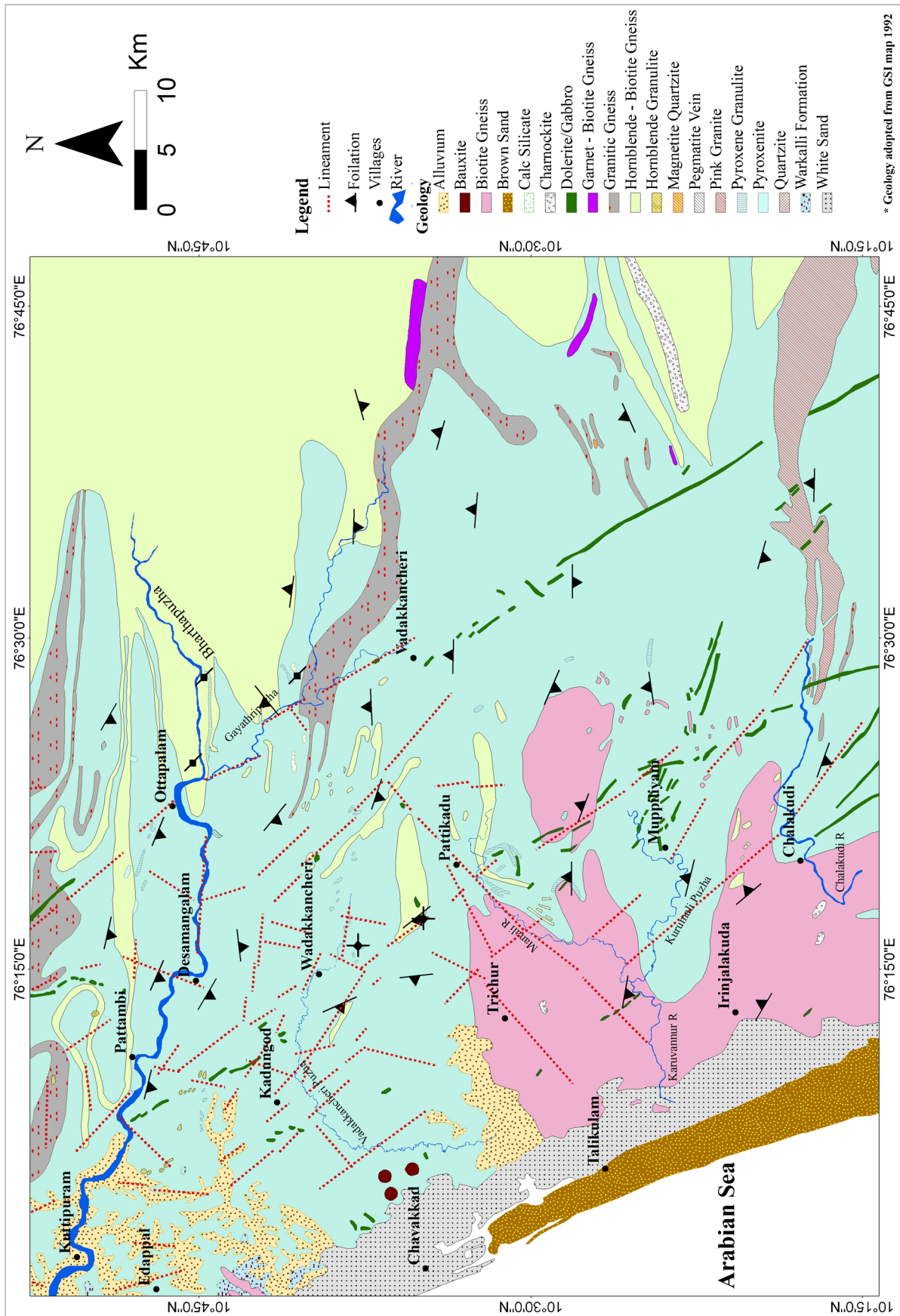


Figure 2. Geological map of the area (geology adopted from GSI 1992). Folded rock units are part of Palghat–Cauvery shear zone. Foliations from the present study are also marked; dotted lines are lineaments identified in the present study.

Bharathapuzha River has less influence on these E–W trending structural elements and is dominated by NW–SE and NE–SW trending structural elements. Central part of the study area shows NW–SE trending dolerite dykes (GSI 1992). It is identified that NW–SE and NNW–SSE lineaments are zones of emplacement of basic dykes related to Deccan volcanism (Krishnaswami 1981; Nair 1990).

The local geology, dominated by a metamorphic suite of charnockite and khondalite group of rocks is shown in figure 2 (GSI 1992). The charnockitic suite of rocks (consisting of granular quartz, feldspar and hypersthene) forms the basement in the area, and is characterized by well-developed foliation, at many places, striking NW–SE with a southward dip of 30°–50°. Quartzo-feldspathic gneiss, pink granite and hornblende biotite gneiss are the other major crystalline rocks in the region (GSI 1992). As per the geological map published by GSI (1992), Warkallai Formation is exposed on the coastal zone between the rivers, Wadakkancheri and Bharathapuzha (figure 2). The higher levels of the crystalline basement are occasionally covered by lateritic regolith and the terraces adjoining the southern bank of the Bharathapuzha River are made up of older alluvium (John 2003).

The NW–SE trending Idamalayar lineament located in the eastern part of the study area is another major structure, which influence the Bharathapuzha River course at Ottapalam (figure 2). Basic dykes are observed along this lineament, south-east of Wadakkancheri (figure 2). Dykes are also observed north of the Bharathapuzha River along the continuity of Idamalayar lineament extending into Palghat–Cauvery shear zone. The Periyar river lineament, which controls the course of the Periyar River for a longer distance (Rajendran *et al.* 2009), also enters through the southern part of the study area. Ghosh *et al.* (2004) considered this as a Precambrian structure and named it as Karur–Kambam–Painavu–Trichur shear zone. This lineament is also associated with basic dykes. Near Muppilayam, a swam of dykes are observed and most of them are in NW–SE direction (figure 2).

3. Methodology

The study area is drained by the rivers, Bharathapuzha, Vadakkancheripuzha, Karuvannur, and Chalakudipuzha and their tributaries. In order to investigate the tectonic influence on landforms of the study area, initially we delineate lineaments from multispectral Landsat images. Drainage network is extracted from topographic maps for morphometric analysis, and it is cross-checked with satellite images. Identification of lineaments, demarcation of drainage system and their

anomalous pattern are carried out through image enhancement and visual interpretation of Landsat image as well as using toposheets.

The special associations of anomalous patterns of drainages with the lineaments are demarcated to understand the influence of lineaments in the drainage system. River sinuosity is calculated for different stretches along the rivers in the area (figure 3), to constrain any change in slope in the river path. To identify anomalies in landscape and drainage system of the area, we have employed morphometric parameters like bifurcation ratio, drainage density, ruggedness number, elongation ratio and asymmetry factor. The Horton's classification of stream order (Horton 1945) is used for the morphometric analysis. The study area is divided into 135 sub-basins having 3rd or 4th order streams and the above-mentioned morphometric parameters are calculated for individual basins (figure 4). The area is further divided into six zones to delineate relative tectonic signatures of the area, if any. The morphometric data are treated from a statistical point of view to determine an average state of the drainage systems to highlight the relative influence of lineaments in each zone.

Further, we have conducted ground-based checks to identify the manifestations of brittle faulting along the lineaments. The structural and lithologic nature of faults is studied to understand its relation to present tectonic regime. Slickensides are plotted as per the procedure suggested by Marshak and Mitra (1988) to identify the movement plane. The earthquake data is further integrated into the study to see their spatial relation with geomorphic anomalies and brittle faults.

4. Drainage network and lineaments set-up of the area

Different stages of tectonic evolutions in Indian craton were documented by Drury and Holt (1980) through analysis of lineament pattern with the help of Landsat imageries. Grady (1971) identified the lineaments trending NNE–SSW to NE–SW as faults that had disturbed the dolerite dykes in south India, which are located outside the study area in the eastern side. Nair (1990) identified five sets of lineaments in the Kerala region, viz., WNW–ESE, NW–SE, NNW–SSE, NNE–SSW, and ENE–WSW.

The Bharathapuzha, Vadakkancheripuzha, Karuvannur and Chalakudipuzha are the major rivers in the area (figure 3). While the Bharathapuzha River is flowing in the northern end of the study area, the Vadakkancheripuzha, Karuvannur and Chalakudi rivers are located to the south. The Karuvannur River has two major tributaries, Manali

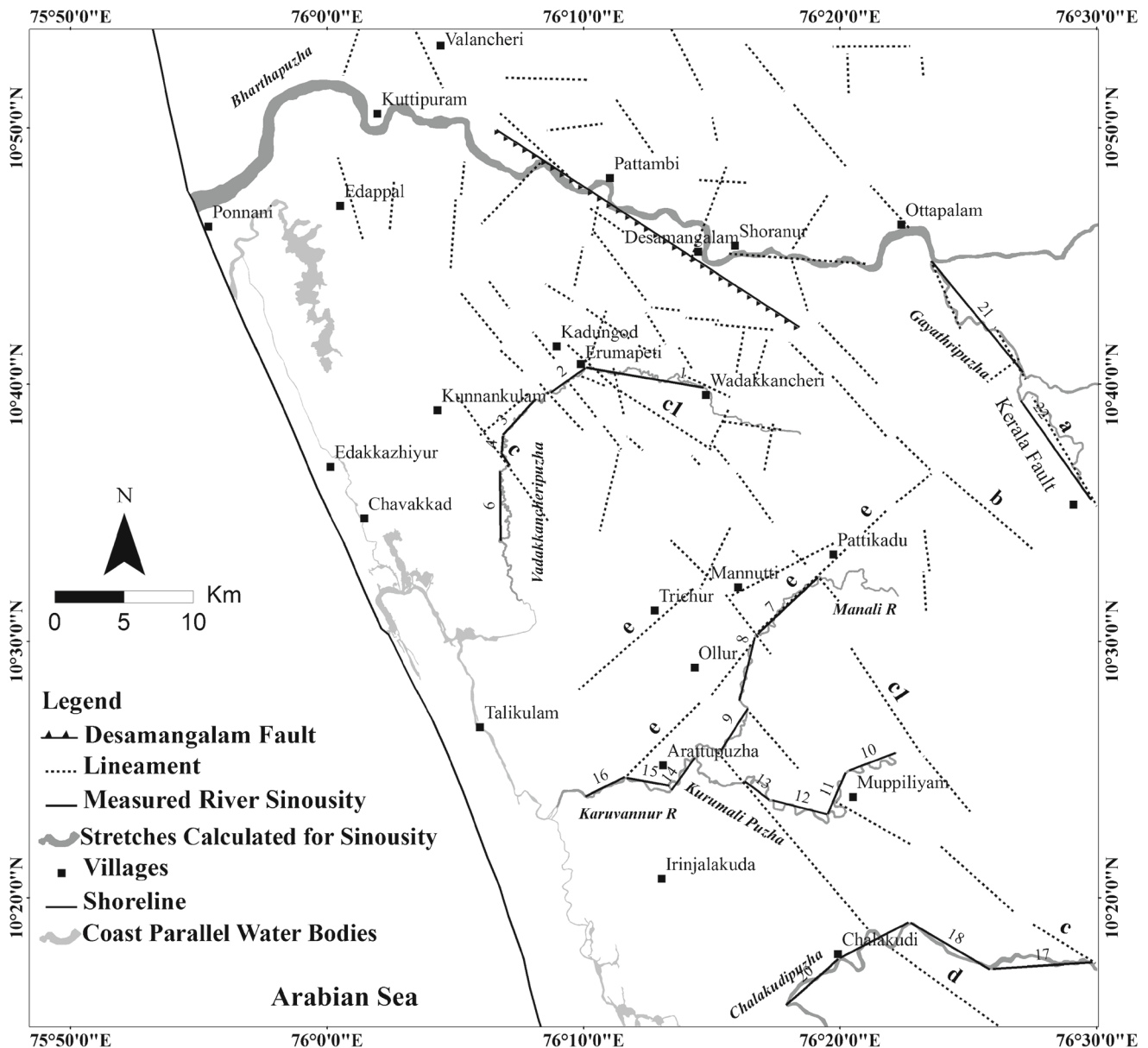


Figure 3. Map showing major rivers of the area and lineaments. Note the change in river direction at the locations where lineament c, c1 and d cross the rivers. Stretches measured for sinuosity are numbered and values are given in table 3.

and Karumalipuzha. Unlike the Bharathapuzha and Chalakkudipuzha rivers that are debouching into sea, the Vadakkancheripuzha and Karuvannur rivers reach the coast as parallel water bodies.

Our study also delineates lineament such as the NW–SE Idamalayar lineament ‘a’ (in figure 1), which is prominent in the eastern side of the area and it has disturbed the Bharathapuzha course at Ottappalam, and it follows the river Gayatripuzha (figure 3). This river, however, shows more meandering flow pattern than the main trunk of the Bharathapuzha in the downstream. Continuation of Idamalayar lineament in the gap overprints on the original E–W trend and appears to have formed later (John 2003). Presence of dolerite dykes along

this lineament, which is dated as 76 Ma (Subrahmaniam 1976), suggest that this lineament may be associated with the initial stages of Deccan volcanism.

A second set of NW–SE trending lineaments (‘b’ in figure 3) is subparallel to Idamalayar lineament, which follows Desamangalam Fault, identified in the previous studies. In the southern side of the area, two sets of NW–SE trending lineaments (‘c’ and ‘d’ in figure 3), appear to be extending from Periyar Fault (in figure 1) and are passing across the rivers Chalakkudi, Kurumalipuzha, Manali and Vadakkancheripuzha (figure 3). A prominent NE–SW trending lineament ‘e’ is identified passing through Pattikadu and Edakunni (figure 3). The

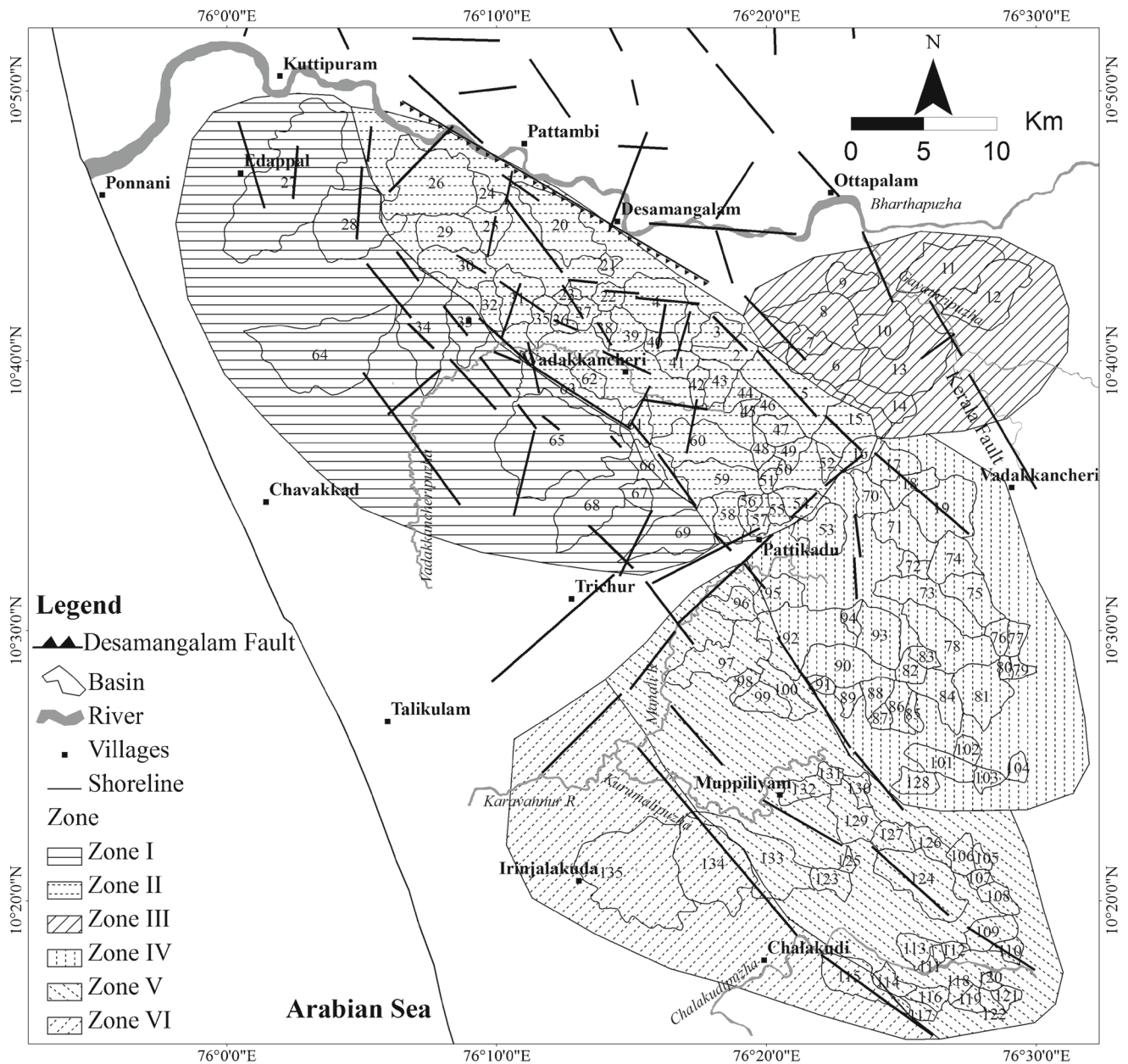


Figure 4. Drainage basins demarcated for morphometric analysis. The six zones, based on the lineaments and topography are also shown. The results are shown in figures 5 and 6.

southwest continuity of this lineament is marked by two subparallel lineaments. However, this lineament appears to be abutting against the lineament ‘b’ at northeast.

5. Geomorphic analysis

The area is mostly low relief and all rivers flow with a gentle gradient in most of its length. Though the rivers are flowing through wide valleys, they exhibit sharp turn and meandering. Some of the earlier studies proved that even the smallest changes in the topography affect the sinuosity of low gradient rivers (Holbrook and Schumm 1999; Schumm 2000). The composition of the stream system of a

drainage basin is expressed quantitatively through stream order, drainage density, bifurcation ratio and stream length ratio (Horton 1945). It incorporates quantitative study of the various components such as stream segments, basin length, basin parameters, basin area, altitude, volume and slopes of the land. The widely accepted objective of morphometric analysis is to find out the drainage characteristic to explain the overall evaluation of the basin. Quantitative measurements of drainage network are also used as a reconnaissance tool to make inferences about relative tectonic activity (e.g., Cox 1994; Keller and Pinter 1996).

The geomorphic indicators, viz., drainage basin asymmetry and sinuosity of river are generally

used to detect active tectonics (Keller and Pinter 1996; Ramasamy *et al.* 2011). Apart from these, the study calculated some conventional geomorphic parameters that are used in hydrologic analysis. The definitions of parameters calculated in the study are given in table 1 and the outcome is shown in figures 5 and 6. The following parameters appear to be significant for understanding the analytical methods, followed by us (table 2).

5.1 River deflections and sinuosity

Under a given set of stable tectonic conditions, alluvial rivers tend to evolve as single meandering channels (Zámolyi *et al.* 2010). If this behaviour is influenced by tectonic movements, it is expected to be reflected in river channel parameters. Within a given range of channel gradients, the meandering pattern changes as vertical tectonic movements influence the valley slope. This process is largely independent of river size, once the fluvial system enters the meandering stage (Zámolyi *et al.* 2010).

River sinuosity is relatively lesser in areas where the valley is narrow and straight. In the study area,

rivers are flowing in NW–SE, N–S and NE–SW directions. Previous studies identified the influence of NW–SE trending lineaments in the E–W course of Bharathapuzha (John and Rajendran 2008). In the present study, 22 stretches on the rivers, namely, Gayathripuzha, Mangalampuzha, Vadakkancheripuzha, Manali, Kurumalipuzha, Karuvanur and Chalakudi, are analysed for sinuosity (figure 3). The river sinuosity values are ranging from 1.6 to 3.38 (table 3). The rivers show changes in directions of flow and sinuosity values on either side of the NW–SE trending lineaments (figure 3). In the southern side of the study area, the Kurumalipuzha River shows compressed meandering between the lineaments ‘c’ and ‘d’. The direction of the Manali River course changes to SW when it crosses the lineament ‘c1’ southwest of Pattikadu. The Vadakkancheripuzha River also shows the same deflection when it crosses near Erumapetti (figure 3). The lineament ‘c’ appears to have induced a sharp turn towards southeast in the Kurumalipuzha River near Muppiliyam. The same lineament appears to have induced sharp deflections towards SE in the river courses of Manali and

Table 1. *Morphometric parameters used in the study.*

Sl. no.	Morphometric parameter	Formula used	Reference
1	Bifurcation ratio (R_b)	$R_b = Nu/Nu + 1$; where Nu = total number of stream segments of order ‘U’, Nu + 1 = number of stream segments of next higher order.	Schumm (1956)
2	Form factor (R_f)	$R_f = A/Lb^2$; where A = area of basin, Lb = length of basin.	Horton (1945)
3	Elongation ratio (R_e)	$R_e = (2/Lb) \times (A/\pi)^{0.5}$	Schumm (1956)
4	Circularity ratio (R_c)	$R_c = 4\pi A/P^2$; where A = area of the basin, P = perimeter of the basin.	Miller (1953)
5	Stream frequency (F_s)	$F_s = Nu/A$; where Nu = total number of streams, A = area of basin.	Horton (1945)
6	Drainage density (DD)	$DD = L/A$; where L = total length of streams of all orders, A = area of basin.	Horton (1945)
7	Constant of channel maintenance (C)	$C = 1/(DD)$; where, DD = drainage density.	Schumm (1956)
8	Basin relief (H)	$H = H_h - H_l$; where H_h = highest elevation in a basin, H_l = lowest elevation in that basin.	Schumm (1956)
9	Ruggedness number(R_n)	$R_n = H \times DD$; where H = basin relief, DD = drainage density.	Schumm (1956)
10	Relief ratio (R_h)	H/Lb ; where H = basin relief, Lb = basin length.	Schumm (1954)
11	Asymmetry factor (AF)	$AF = 100 \times (Ar/At)$; where Ar = right half of area of basin while facing downstream, At = total area of the basin.	Keller and Pinter (1996)
12	Sinuosity of river (S)	$S = L_C/L_V$ where L_C = channel length, L_V = valley length.	Schumm (2000)

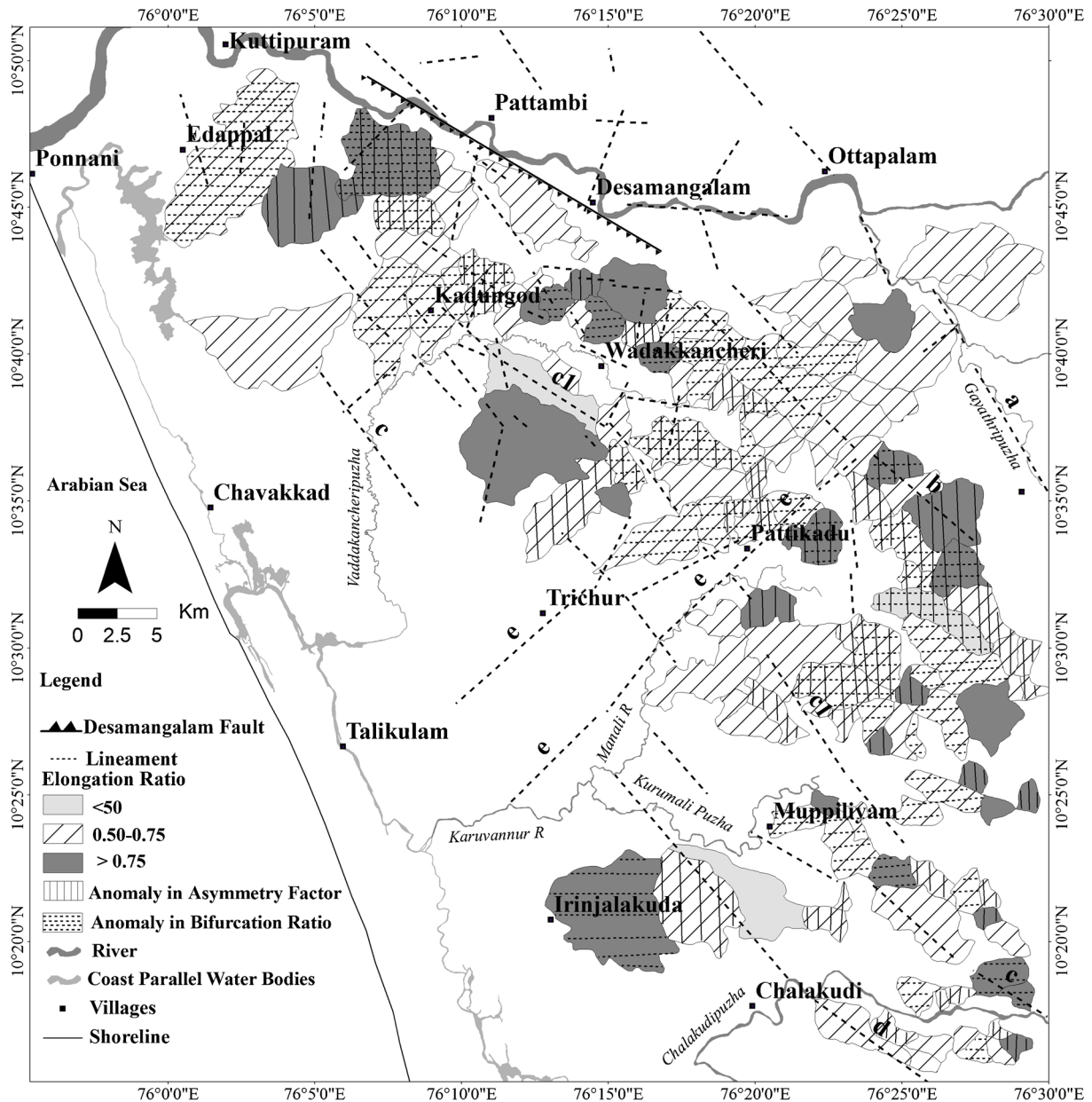


Figure 5. Map showing spatial distribution of elongation ratio as well as anomalies in bifurcation ratio and asymmetry factor in different basins. Horizontal dashed lines represent basins with bifurcation ratio values higher than 3; vertical solid lines represent anomalously high values of basin asymmetry.

Vadakkancheripuzha rivers, southeast of Edakkuni and Kunnamkulam, respectively (figure 3).

Those drainage segments showing change in directions and drastic change in sinuosity values compared to subsequent segments represent anomalies. As mentioned earlier, features, such as change in slope, are generally considered as structurally controlled and is a strong evidence for the presence of active faults/neotectonic lineaments. Comparison of the sinuosity distribution along the river courses with geological and geomorphological features that changes in sinuosity values reflecting neotectonic features (Zámolyi et al. 2010). In

peninsular India too similar features are attributed to active faults (Ramasamy et al. 2011).

5.2 Bifurcation ratio (R_b)

Horton (1945) considered bifurcation ratio as an index of relief and dissections. Strahler (1951) found that bifurcation ratio shows only slight variation in different zones except where the powerful geological controls dominate. The R_b characteristically ranges between 3.0 and 5.0 for the basins in which the geologic structure does not affect the drainage pattern (Strahler 1964). In the present

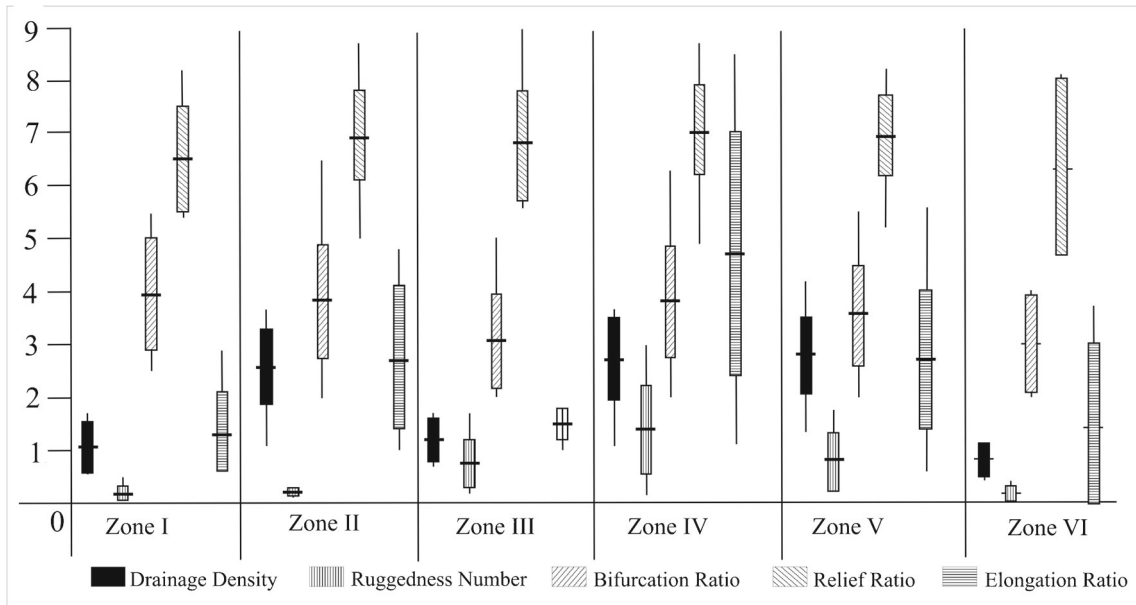


Figure 6. Sample range diagram representing the morphometric parameters DD, R_b , R_n , R_e and relief ratio for different zones. The bar represents the data range within standard deviation; the horizontal lines at the centre of the bars represent the average values; vertical lines are connecting maximum and minimum.

study, R_b for 135 sub-basins has been calculated based on the formula shown in table 1. The mean value of the R_b between first and second order streams for 135 sub-basins is found to be 3.68 (table 2). The high values of R_b are an indication of terrain rejuvenation due to young tectonic movements (Zuchiewicz 1989; Panek 2004). The present study shows that higher R_b is mostly confined to basins located in high relief (figures 5 and 6). However, there are basins in low relief area that show high values of R_b and most of them are located between the Bharathapuzha and Vadakkancheripuzha rivers, where the lineaments are more segmented (figure 5). This could be due to the recent activity along these NW–SE trending lineaments.

5.3 Drainage density (DD)

The DD expresses the closeness of spacing of channels and it depends on the characteristics such as soil type, rock type, vegetation strength, climate and infiltration strength (Strahler 1957). A low DD is more likely to occur in regions of highly resistant or highly permeable subsoil material under dense vegetative cover and where relief is low. High DD is the resultant of weak or impermeable subsurface material, sparse vegetation and mountainous relief (Strahler 1964). In the present study, the DD is calculated based on the formula shown in table 1, and it varies between 0.38 and 4.16 (table 2). The mean value of the DD for the area is 2.34. It is found that higher drainage densities are associated with high relief of the basins and are mainly confined to b and c1 lineaments (figure 6a).

5.4 Ruggedness number (R_n)

This parameter combines the slope steepness of the basin with its length (Strahler 1964; table 1). Higher the basin relief, higher will be the values of R_n . This condition is expected in tropical climate areas with high rainfall (Schumm 1956). The value of R_n within the study area varies from 0.01 to 2.98 with the mean value of 0.80 (table 2). If we consider that 0.5 to 1.5 is the normal range of values of R_n within the study area, 52 basins are falling in this range. However, only 20 basins are falling above this range of values. Like DD, higher values of R_n are associated with high relief of the basins and cannot be considered as anomalous (figure 6).

5.5 Elongation ratio (R_e)

The range of R_e is, in general, between 0 and 1, and it can be classified as into elongated, less elongated, oval and circular (Schumm 1956). It is observed that values close to 1 are in regions of very low relief and values between 0.6 and 0.8 are associated with regions of high relief and steep ground slope (Strahler 1964). There are also attempts to classify tectonic activity based on the values on R_e (Zuchiewicz 2001). In the study area, the R_e of the basins ranges between 0.48 and 0.90 (table 2). The study shows that only 29 basins are falling in the values less than 0.5 and for 103 basins the value ranges between 0.5 and 0.7, which indicate the basins are relatively elongated (figure 5). Higher elongation ratio is also observed in areas of low relief (figure 6). The most anomalous

Table 2. Drainage basin parameters derived for the study area.

Basin no.	Bifurcation ratio f/s	Form factor	Elongation ratio	Circularity ratio	Stream frequency	Drainage density	Ccm	Basin relief	Ruggedness number	Relief ratio	Asymmetry factor
1	6.50	0.39	0.70	0.61	3.95	2.44	0.41	0.302	0.74	0.0935	41.81
2	4.75	0.26	0.58	0.51	4.42	2.72	0.37	0.303	0.83	0.0664	29.13
3	4.50	0.41	0.72	0.72	2.24	1.58	0.63	0.282	0.45	0.0779	57.41
4	2.50	0.56	0.85	0.79	0.60	0.69	1.45	0.32	0.22	0.0657	44.84
5	4.33	0.37	0.69	0.54	3.38	2.48	0.40	0.462	1.15	0.0630	59.86
6	5.00	0.32	0.64	0.54	1.29	1.54	0.65	0.162	0.25	0.0289	59.61
7	2.50	0.44	0.75	0.63	2.24	1.67	0.60	0.118	0.20	0.0413	65.53
8	3.50	0.25	0.57	0.48	0.74	1.07	0.93	0.182	0.19	0.0248	40.96
9	3.50	0.41	0.72	0.67	1.89	1.41	0.71	0.169	0.24	0.0471	35.56
10	3.00	0.63	0.90	0.69	1.26	1.67	0.60	0.175	0.29	0.0433	41.89
11	2.50	0.29	0.61	0.54	0.47	0.69	1.45	0.167	0.11	0.0220	45.30
12	2.00	0.36	0.68	0.54	0.42	0.64	1.56	0.102	0.07	0.0151	44.96
13	3.00	0.37	0.69	0.56	0.48	0.93	1.08	0.175	0.16	0.0247	51.84
14	2.50	0.23	0.54	0.49	1.08	1.00	1.00	0.12	0.12	0.0212	43.15
15	3.50	0.40	0.71	0.63	0.84	1.04	0.96	0.462	0.48	0.0844	59.00
16	4.00	0.41	0.72	0.74	2.19	1.90	0.53	0.28	0.53	0.0797	62.59
17	2.50	0.46	0.77	0.67	1.27	1.02	0.98	0.38	0.39	0.1030	19.96
18	3.00	0.34	0.66	0.52	1.73	1.76	0.57	0.36	0.63	0.0916	59.26
19	2.75	0.54	0.83	0.66	1.06	1.06	0.95	0.105	0.11	0.0198	31.75
20	3.33	0.25	0.57	0.46	0.90	1.13	0.89	0.162	0.18	0.0207	41.67
21	3.00	0.45	0.76	0.64	6.01	2.58	0.39	0.12	0.31	0.0659	39.13
22	2.67	0.60	0.87	0.74	3.68	2.59	0.39	0.1	0.26	0.0427	27.90
23	3.00	0.38	0.70	0.59	5.45	3.26	0.31	0.15	0.49	0.0720	50.36
24	2.00	0.38	0.70	0.61	2.00	1.43	0.70	0.101	0.14	0.0333	42.80
25	2.50	0.43	0.74	0.57	1.30	1.36	0.74	0.101	0.14	0.0268	42.16
26	4.50	0.53	0.82	0.58	0.91	1.24	0.81	0.121	0.15	0.0175	67.79
27	5.33	0.31	0.63	0.46	0.41	0.65	1.53	0.08	0.05	0.0064	53.10
28	3.50	0.53	0.82	0.67	0.47	0.90	1.11	0.068	0.06	0.0107	29.82
29	5.50	0.44	0.75	0.70	1.55	1.40	0.71	0.1	0.14	0.0219	24.45
30	3.00	0.34	0.66	0.58	1.34	1.51	0.66	0.14	0.21	0.0263	58.63
31	5.80	0.45	0.75	0.59	3.74	2.50	0.40	0.18	0.45	0.0392	81.71
32	6.00	0.31	0.63	0.57	3.74	2.78	0.36	0.16	0.44	0.0445	52.47
33	5.50	0.31	0.62	0.60	1.31	1.28	0.78	0.16	0.20	0.0271	61.09
34	4.00	0.27	0.58	0.54	0.56	1.04	0.96	0.14	0.15	0.0163	55.86
35	3.50	0.32	0.64	0.57	4.35	2.48	0.40	0.18	0.45	0.0490	55.66
36	3.50	0.45	0.76	0.69	3.95	2.36	0.42	0.14	0.33	0.0593	42.47
37	4.50	0.59	0.87	0.70	3.51	2.70	0.37	0.12	0.32	0.0498	46.73
38	3.00	0.36	0.67	0.61	5.16	2.89	0.35	0.122	0.35	0.0458	38.46
39	6.00	0.52	0.82	0.68	4.10	2.72	0.37	0.17	0.46	0.0531	84.74
40	2.75	0.41	0.73	0.70	5.17	2.87	0.35	0.28	0.80	0.1024	16.83
41	5.00	0.48	0.78	0.81	4.58	2.92	0.34	0.36	1.05	0.1220	62.77
42	2.25	0.33	0.65	0.65	5.02	2.76	0.36	0.36	1.00	0.1243	55.07
43	4.60	0.44	0.75	0.55	5.85	2.93	0.34	0.36	1.05	0.1037	48.36
44	3.00	0.36	0.68	0.53	7.16	3.05	0.33	0.3	0.91	0.1011	27.85
45	2.00	0.28	0.60	0.57	8.36	2.88	0.35	0.28	0.81	0.1630	29.87
46	4.00	0.39	0.71	0.52	6.57	3.49	0.29	0.385	1.34	0.1550	23.00
47	3.67	0.40	0.72	0.74	3.02	2.48	0.40	0.43	1.07	0.1225	58.53
48	5.00	0.29	0.60	0.59	4.81	2.74	0.37	0.36	0.98	0.1172	43.68
49	3.33	0.39	0.70	0.60	4.80	3.09	0.32	0.422	1.31	0.1533	59.94
50	2.50	0.27	0.58	0.46	7.74	3.03	0.33	0.34	1.03	0.1733	75.00
51	3.00	0.44	0.75	0.79	5.78	3.17	0.32	0.362	1.15	0.1931	66.65
52	3.50	0.26	0.58	0.53	4.47	2.73	0.37	0.38	1.04	0.1304	53.68
53	4.17	0.55	0.84	0.67	3.63	2.60	0.38	0.38	0.99	0.0954	65.19

Table 2. (Continued.)

Basin no.	Bifurcation ratio f/s	Form factor	Elongation ratio	Circularity ratio	Stream frequency	Drainage density	Ccm	Basin relief	Ruggedness number	Relief ratio	Asymmetry factor
54	4.00	0.37	0.68	0.66	3.83	2.97	0.34	0.475	1.41	0.1227	38.95
55	4.00	0.40	0.72	0.70	4.90	3.07	0.33	0.475	1.46	0.2016	79.67
56	4.00	0.30	0.62	0.45	6.66	3.55	0.28	0.46	1.63	0.1638	28.50
57	4.00	0.30	0.62	0.51	5.70	3.53	0.28	0.47	1.66	0.1539	46.79
58	4.80	0.39	0.71	0.57	5.83	3.09	0.32	0.4	1.24	0.1068	44.01
59	3.25	0.28	0.60	0.50	3.08	2.50	0.40	0.46	1.15	0.0728	60.56
60	4.29	0.25	0.56	0.45	2.71	1.87	0.53	0.38	0.71	0.0503	21.44
61	3.50	0.40	0.71	0.60	3.59	1.62	0.62	0.15	0.24	0.0410	57.44
62	3.20	0.35	0.67	0.64	6.51	3.62	0.28	0.12	0.43	0.0387	69.86
63	3.71	0.19	0.50	0.34	2.55	2.00	0.50	0.152	0.30	0.0175	47.07
64	2.50	0.32	0.64	0.56	0.23	0.62	1.61	0.058	0.04	0.0056	38.59
65	3.50	0.47	0.77	0.55	0.52	0.88	1.14	0.12	0.11	0.0129	51.85
66	4.00	0.35	0.66	0.59	4.55	2.78	0.36	0.13	0.36	0.0356	32.47
67	3.00	0.45	0.76	0.76	2.89	2.34	0.43	0.14	0.33	0.0534	36.51
68	3.00	0.26	0.58	0.43	1.92	1.72	0.58	0.14	0.24	0.0173	65.62
69	4.20	0.23	0.54	0.47	1.96	1.63	0.61	0.29	0.47	0.0376	53.68
70	3.75	0.35	0.67	0.60	3.73	2.69	0.37	0.34	0.91	0.0872	28.70
71	4.50	0.38	0.69	0.57	1.33	1.15	0.87	0.149	0.17	0.0305	12.87
72	4.00	0.44	0.75	0.60	4.09	2.54	0.39	0.184	0.47	0.0745	78.32
73	5.20	0.19	0.49	0.39	2.68	2.22	0.45	0.42	0.93	0.0531	32.09
74	4.50	0.53	0.82	0.64	1.53	1.56	0.64	0.16	0.25	0.0416	73.81
75	2.83	0.32	0.64	0.59	2.96	2.33	0.43	0.433	1.01	0.0864	75.65
76	3.50	0.40	0.71	0.69	3.57	2.72	0.37	0.848	2.31	0.3202	65.33
77	3.33	0.38	0.69	0.65	5.32	3.51	0.28	0.848	2.98	0.3203	31.79
78	4.18	0.27	0.59	0.48	3.91	3.11	0.32	0.82	2.55	0.1089	64.79
79	3.00	0.39	0.71	0.58	5.68	3.38	0.30	0.52	1.76	0.2596	29.04
80	2.00	0.44	0.75	0.73	7.65	3.60	0.28	0.6	2.16	0.3487	64.72
81	3.89	0.47	0.78	0.69	4.02	2.94	0.34	0.78	2.30	0.1570	55.03
82	3.00	0.46	0.76	0.67	4.13	2.77	0.36	0.355	0.98	0.1355	73.99
83	5.50	0.36	0.68	0.74	6.45	3.61	0.28	0.26	0.94	0.1057	46.55
84	5.20	0.31	0.63	0.47	4.18	3.17	0.32	0.815	2.58	0.1636	51.61
85	4.00	0.24	0.55	0.52	5.81	3.19	0.31	0.34	1.09	0.1201	64.81
86	3.67	0.27	0.59	0.49	3.65	2.88	0.35	0.74	2.13	0.1911	53.99
87	3.50	0.59	0.87	0.84	4.92	2.90	0.35	0.614	1.78	0.3308	34.94
88	5.67	0.39	0.71	0.68	5.38	3.40	0.29	0.76	2.59	0.2406	36.01
89	3.00	0.40	0.71	0.59	5.14	3.01	0.33	0.614	1.85	0.2446	71.28
90	6.29	0.29	0.61	0.57	4.50	3.09	0.32	0.74	2.28	0.1160	31.70
91	3.00	0.45	0.76	0.79	6.19	3.13	0.32	0.315	0.98	0.1755	52.80
92	3.71	0.40	0.71	0.48	3.60	2.39	0.42	0.45	1.07	0.0644	40.11
93	4.20	0.37	0.69	0.72	2.67	2.37	0.42	0.637	1.51	0.1217	32.80
94	2.50	0.32	0.64	0.53	4.06	2.26	0.44	0.22	0.50	0.0882	72.65
95	3.50	0.48	0.78	0.68	1.51	1.21	0.83	0.157	0.19	0.0422	72.38
96	3.83	0.37	0.69	0.59	5.85	3.07	0.33	0.157	0.48	0.0409	35.84
97	2.60	0.27	0.59	0.32	1.22	1.29	0.78	0.21	0.27	0.0278	61.70
98	2.50	0.31	0.62	0.54	3.66	2.18	0.46	0.21	0.46	0.0786	60.07
99	3.67	0.36	0.68	0.67	2.66	2.01	0.50	0.2	0.40	0.0508	38.18
100	3.00	0.21	0.52	0.39	2.30	2.09	0.48	0.19	0.40	0.0368	27.67
101	5.33	0.27	0.58	0.59	5.75	3.56	0.28	0.365	1.30	0.0722	45.40
102	3.00	0.53	0.82	0.86	3.54	2.82	0.35	0.321	0.90	0.1464	66.79
103	4.00	0.52	0.82	0.69	4.57	3.09	0.32	0.353	1.09	0.1648	45.63
104	2.50	0.50	0.80	0.77	3.63	3.04	0.33	0.679	2.07	0.3223	80.35
105	2.50	0.41	0.72	0.72	4.89	3.07	0.33	0.243	0.75	0.1210	30.02
106	5.50	0.44	0.75	0.74	3.75	2.69	0.37	0.355	0.96	0.1214	60.96
107	3.50	0.47	0.78	0.77	6.01	3.13	0.32	0.261	0.82	0.1390	19.61

Table 2. (Continued.)

Basin no.	Bifurcation ratio f/s	Form factor	Elongation ratio	Circularity ratio	Stream frequency	Drainage density	Ccm	Basin relief	Ruggedness number	Relief ratio	Asymmetry factor
108	3.50	0.37	0.68	0.72	5.04	3.19	0.31	0.536	1.71	0.1669	61.20
109	5.00	0.47	0.77	0.77	4.02	2.79	0.36	0.556	1.55	0.1527	60.66
110	5.00	0.53	0.82	0.64	5.32	2.98	0.34	0.34	1.01	0.1588	38.24
111	2.00	0.41	0.73	0.75	8.41	4.00	0.25	0.4	1.60	0.2820	77.08
112	3.00	0.42	0.73	0.73	8.18	4.16	0.24	0.4	1.66	0.2060	16.97
113	4.00	0.44	0.75	0.62	3.95	2.68	0.37	0.42	1.13	0.1390	64.84
114	2.50	0.36	0.68	0.60	2.39	1.84	0.54	0.08	0.15	0.0262	83.15
115	2.50	0.21	0.51	0.47	0.77	1.08	0.93	0.1	0.11	0.0141	58.46
116	3.00	0.34	0.66	0.61	5.55	2.54	0.39	0.06	0.15	0.0201	43.37
117	3.33	0.27	0.59	0.54	6.70	3.25	0.31	0.08	0.26	0.0289	49.53
118	3.00	0.41	0.72	0.75	5.15	3.04	0.33	0.28	0.85	0.1355	53.05
119	5.00	0.44	0.75	0.66	5.59	3.11	0.32	0.288	0.90	0.1253	36.53
120	3.50	0.42	0.73	0.58	8.98	3.79	0.26	0.362	1.37	0.2217	83.16
121	3.00	0.46	0.77	0.70	6.31	3.87	0.26	0.342	1.32	0.1624	25.90
122	3.50	0.30	0.62	0.64	5.54	3.66	0.27	0.268	0.98	0.1090	57.21
123	3.00	0.44	0.75	0.71	2.12	2.04	0.49	0.3	0.61	0.0964	67.10
124	3.33	0.35	0.67	0.60	1.54	1.56	0.64	0.395	0.62	0.0558	61.91
125	2.00	0.32	0.64	0.54	6.90	3.37	0.30	0.3	1.01	0.1683	32.53
126	3.33	0.24	0.56	0.50	3.34	2.44	0.41	0.36	0.88	0.0866	76.15
127	4.67	0.51	0.80	0.69	3.88	2.64	0.38	0.197	0.52	0.0650	36.30
128	4.75	0.40	0.72	0.69	6.24	3.47	0.29	0.326	1.13	0.1013	35.21
129	5.33	0.41	0.72	0.58	2.24	1.86	0.54	0.119	0.22	0.0255	60.14
130	4.50	0.29	0.61	0.43	5.03	2.65	0.38	0.101	0.27	0.0352	55.80
131	3.00	0.51	0.80	0.72	4.76	2.24	0.45	0.1	0.22	0.0518	58.58
132	4.00	0.34	0.66	0.60	2.45	1.82	0.55	0.14	0.25	0.0386	46.37
133	3.50	0.18	0.48	0.36	0.56	0.99	1.01	0.368	0.37	0.0374	56.25
134	2.00	0.42	0.73	0.68	0.29	0.65	1.54	0.08	0.05	0.0106	65.15
135	4.00	0.51	0.81	0.59	0.28	0.38	2.60	0.02	0.01	0.0023	53.53

values for basin elongation of the area (<0.5) is observed along basins oriented in NW–SE direction (figure 5). This further confirms the influence of NW–SE lineaments in the drainage system.

5.6 Asymmetry factor (AF)

For a stream network flowing in a stable setting and uniform lithology, the AF (table 1) should be equal to 50. In all other cases, there will be a change in value deviating on either side of 50 (Keller and Pinter 1996). This factor is used to detect the tectonic tilt of the basin areas (Hare and Gardner 1985). The value for AF is calculated for sub-basins, and the value ranges from 12.87 to 84.74 and the mean is 50.26 (table 2). If we consider that 40–60 is the normal range of values of AF for the study area, only 54 basins are falling in the normal range and 81 basins are showing higher AF (either <40 or >60). The higher and lower values are considered as anomalies and may suggest geological or structural influence. The basins showing higher anomalies in symmetry in the present study area are mostly located between lineaments

b and c1, as well as between c and d (figure 5) and may be indicating tectonic adjustment along these lineaments.

6. Field observations on faults

Initially brittle faults were identified along Desamangalam Fault in which multiple deformations were identified (John and Rajendran 2005). In the present study, lineaments are mostly checked wherever fresh surface of charnockite bed rock is exposed through quarrying. In the study area, the charnockite rocks exhibit occasional NW–SE trending foliations. Thin covers of lateritic soil are present at many places in these exposures. Signature of the NW–SE trending lineament is traced as faults at three locations, viz., Erumapetti, Tayyur and Mannuthi (figure 8). The brittle deformation exposures are associated with damage zone, gouge formation and slickensides. Three types of lithologies can also be distinguished in each of these fault exposures namely: (1) protolith or host rock, (2) damage zone, and (3) a fault core (e.g., Caine

Table 3. Sinuosity index measured along different stretches of rivers in the study area.

	Name of river	Straight length (km)	Curved length (km)	Sinuosity of river
1	Vadakkancheripuzha	6.8	17	2.5
2	Vadakkancheripuzha	4.4	11	2.5
3	Vadakkancheripuzha	3.3	7	2.121
4	Vadakkancheripuzha	1.05	2.99	2.85
5	Vadakkancheripuzha	1.05	1.90	1.81
6	Vadakkancheripuzha	3.5	10	2.857
7	Manalipuzha	5.9	14	2.372
8	Manalipuzha	3.6	8	2.222
9	Manalipuzha	3.9	10	2.564
10	Karumalipuzha	3.7	11	2.972
11	Karumalipuzha	3.25	11	3.384
12	Karumalipuzha	3.96	12	3.030
13	Karumalipuzha	2.41	8	3.319
14	Karuvannurpuzha	2.47	7	2.834
15	Karuvannurpuzha	3.21	8	2.492
16	Karuvannurpuzha	3.13	6	1.916
17	Chalakkudi river	7.2	15	2.083
18	Chalakkudi river	6.4	13	2.031
19	Chalakkudi river	5.53	18	3.254
20	Chalakkudi river	4.73	11	2.325
21	Gayathripuzha	10.6	25	2.358
22	Mangalampuzha	7.45	20	2.6845

et al. 1996; John and Rajendran 2009). Protolith is the undeformed host rock (charnockite) surrounding the fault rock and the damaged zone. The damage zone consists of a network of fault-related subsidiary structures that bound the fault core. The fault related subsidiary structures in the damaged zone include small offsets, veins, fractures and cleavages (Bruhn *et al.* 1994). Fault core is the portion of a fault zone where much of the displacement is accommodated (Caine *et al.* 1996). In the following section, we will present the dominant features at each of the sites.

Erumapetti: The NW–SE trending south dipping fault is traced in a 30 m vertical section (figure 7a) and about 100 m along strike direction in the adjacent quarry. The fault shows varying thickness of damage zone in the vertical section. The thickness of the damage zone is maximum at the bottom (deeper level) and is associated with green-coloured gouge. A number of joints are observed perpendicular to the fault mainly at the top portion. No major subparallel fractures are observed away from the damage zone. Coulomb shears, indicative of slip movement is also observed in the damage zone (figure 7b). Variation in thickness of damage zone is also observed along strike length at the top (figure 7c). Thickness of the fault core also increases towards upper levels.

Tayyur: The lineament ‘c1’ is traced as a brittle fault in another 25 m high quarry face near Tayyur. Here the brittle faulting is marked by closely spaced fractures and gouge (figure 7d). Width of the damage zone is very high compared to that of Erumapetti but the thickness of fault core is less. The damage zone is dominated by fault parallel fractures (figure 7d). Green coloured gouge along with well rounded fine-grained quartz are found along the slip plane (figure 7e). Though water is percolating along the fault, no leaching is observed along any of the fractures within the fault zone.

Mannuti: Another prominent NW–SE trending southwest dipping fault is observed in a charnockite quarry near Mannuti (figure 7f). This fault is lying within the zone of ‘c1’. The width of the damage zone is ~1.5 m. Water seepage is observed along the fault zone and vegetation has grown along it (figure 7g). Rock fragments are also observed within the fault zone, while at the lower portion closely spaced joints are observed parallel to the fault plane within the damage zone. About 300 m further northwest, this fault is again traced in the road cutting along the strike direction 200 m southeast. At the top end of the fault, hanging wall side is more intact than footwall side (figure 7h).

The brittle deformations identified also show development of slickensides. The fault movements

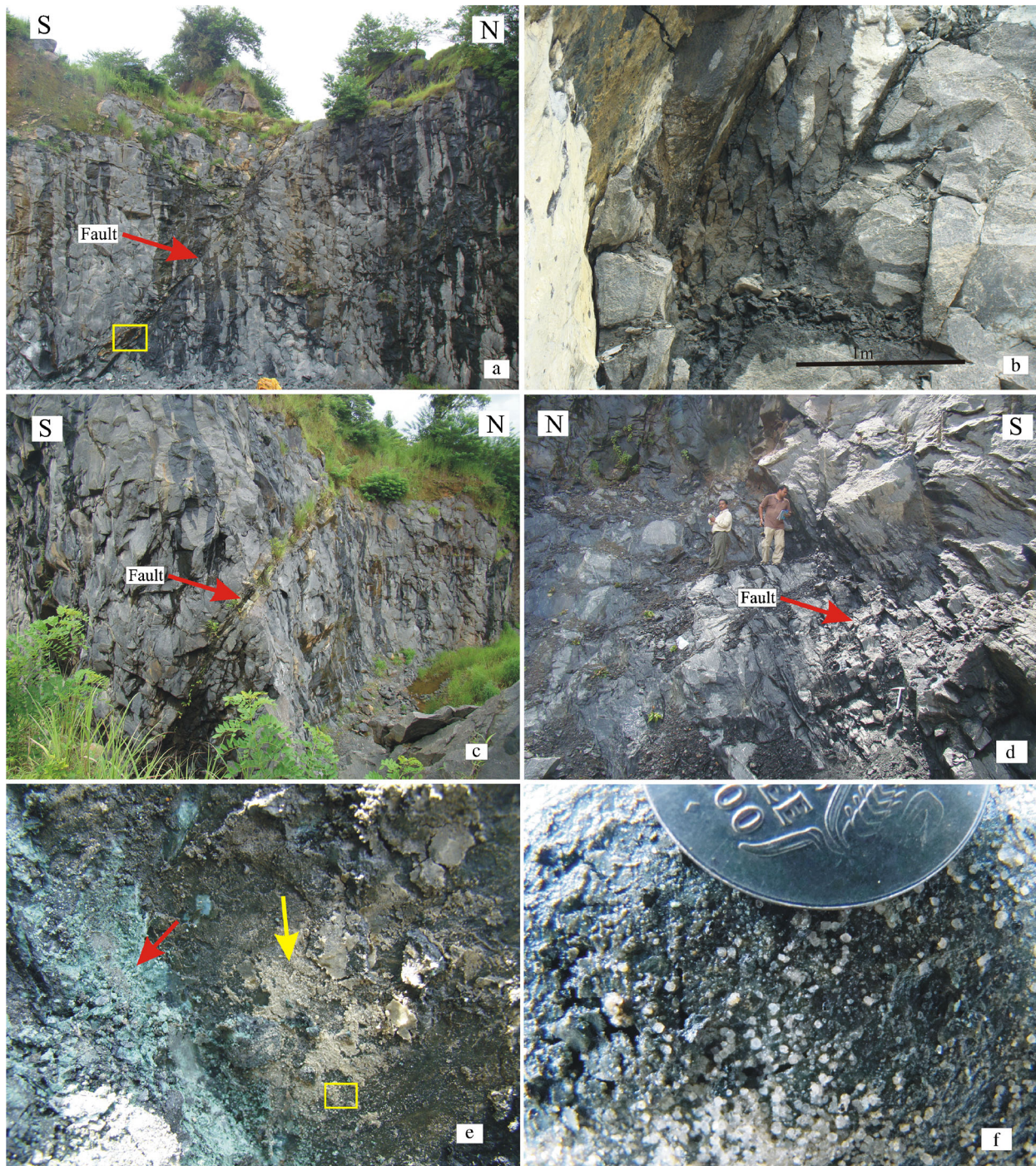


Figure 7. (a) The NW–SE trending brittle fault identified near Erumapetti. The quarry face is about 30 m high; the fault zone showing varying thickness of damage zone from top to bottom. Joints and fractures perpendicular to the fault dominate the upper portion of footwall block; in the hanging wall block such joints appear to be turning towards the fault direction near the slip plane. The area marked in rectangle is shown in (b). (b) The style of damage observed in the bottom portion of the fault mapped, gouge observed on either side of the damaged mass; closely spaced fractures are coulomb joints developed due to the movement. (c) Continuation of the fault in (a) about 100 m northwest of the previous location; note the thick gouge zone near the surface facilitate the growth of vegetation. (d) Brittle faulting observed in a charnockite quarry near Tayoor; note the closely spaced joints parallel observed in the fault zone; the tallest person in the photo is 170 cm high. (e) View of the slip plane in the fault zone shown in (d); two types of gouge observed, shown in green and white. Close look at the gouge of the area marked in rectangle is shown in (f). (f) Close view of white coloured gouge shown in (e), indicating rounded fine-grained quartz. One rupee coin is kept for scale. (g) View of the NW–SE trending south dipping fault observed near Mannuthi; the central part of the quarry advanced towards NW direction. Close-up view of the fault marked in rectangle is shown in (h). (h) Close view of fault core and damage zone marked in (g); note the vegetation grown along the fault core. (i) Tip of the fault zone near Mannuthi; note the relatively intact hanging wall block sitting over a highly crushed and altered footwall.

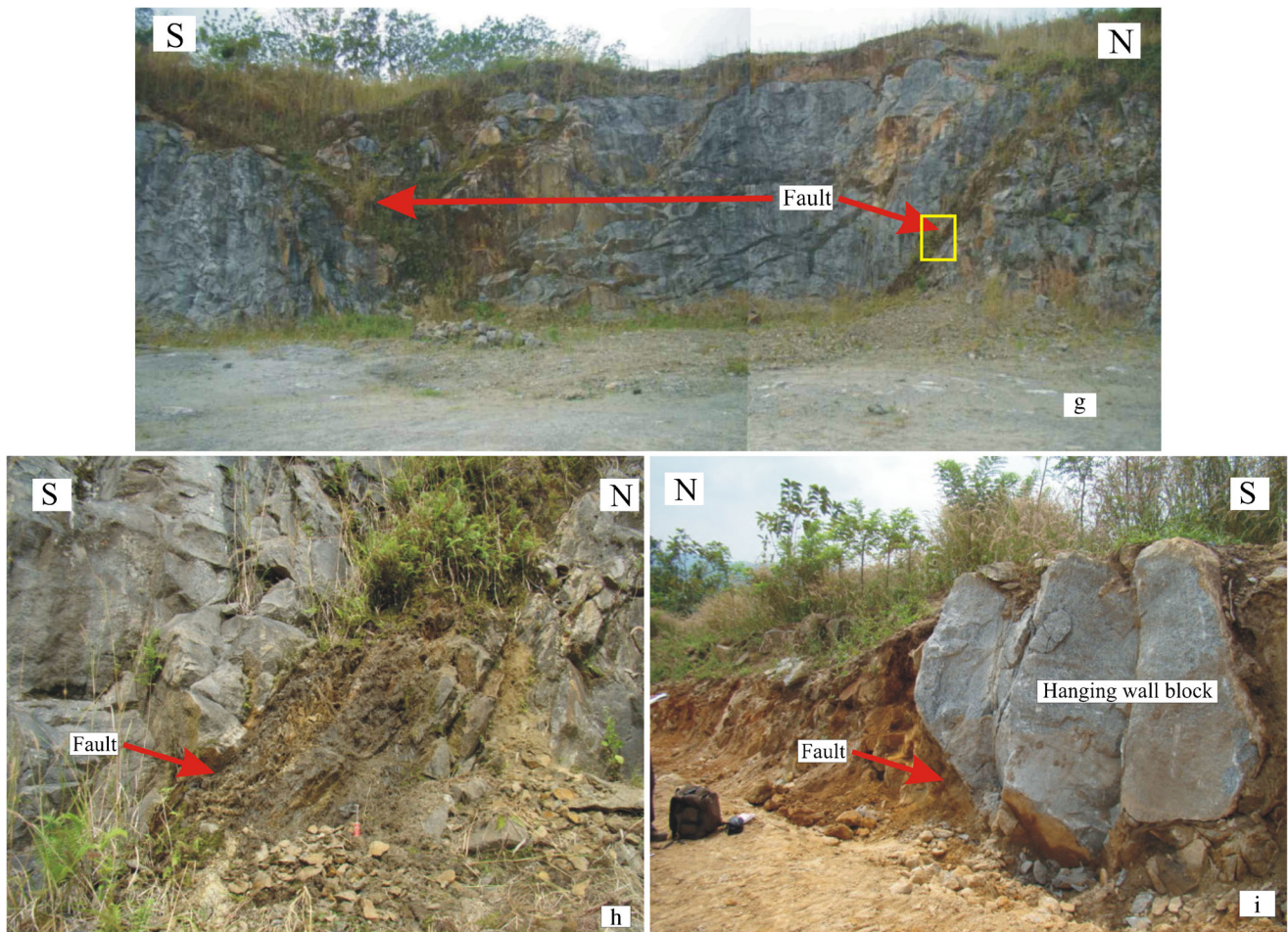


Figure 7. (Continued.)

are dominated with reverse and strike slip movement. However, the amount of slip could not be measured at these places due to the lack of marker beds across these faults. The movement directions across the faults are evaluated from slickensides by using the technique suggested by Marshak and Mitra (1988), in which movement planes are calculated by plotting fault planes and slickensides. The results show that the movement plane constructed on slip surfaces indicate oblique movement (figure 8). In all cases, the southwestern blocks are moving towards north or northeast (figure 8).

7. Seismicity of the area

Among the historic and recent earthquakes of the region, 1900 Coimbatore earthquake is significant in south India (Basu 1964). A large number of tremors have been reported in the vicinity of Palghat Gap in the recent past (Rajendran and Rajendran 1996). The biggest of them (M 4.3) is located at 10.75°N and 76.25°E (Rajendran and Rajendran 1995), and its isoseismal elongation is spatially coincide with the Desamangalam Fault

(John 2003). This earthquake made widespread minor damages to houses around the epicentral area (intensity V), mostly confined to south of Bharathapuzha. Most of the aftershocks detected by IMD network (IMD 1995) are also located close to the above said structure (John 2003). Subsequent mild activity was reported further south of the 1994 event (Rajendran *et al.* 2009) along the branches of Periyar lineament (figure 8).

On the southeastern terminus of Periyar lineament, an earthquake of M 4.5 was reported on 09.06.1988 (figure 1), which was followed by several aftershocks (Singh *et al.* 1989). This earthquake was felt in about 50 km radius, and caused damage to buildings in the epicentral area and was assigned a maximum intensity VI. Mishra *et al.* (1989) based on gravity studies, identified a shallow structure corresponding to Periyar Fault in that area. The composite fault plane solution suggests its association with Periyar Fault (Rastogi *et al.* 1995).

During April–July 2012, another swarm of earthquake events occurred southeast of Wadakkancheri. The biggest event M = 3.8 occurred on 19.07.2012 near Tannikulam, as recorded in Peechi Observatory. Many such local events are plotted

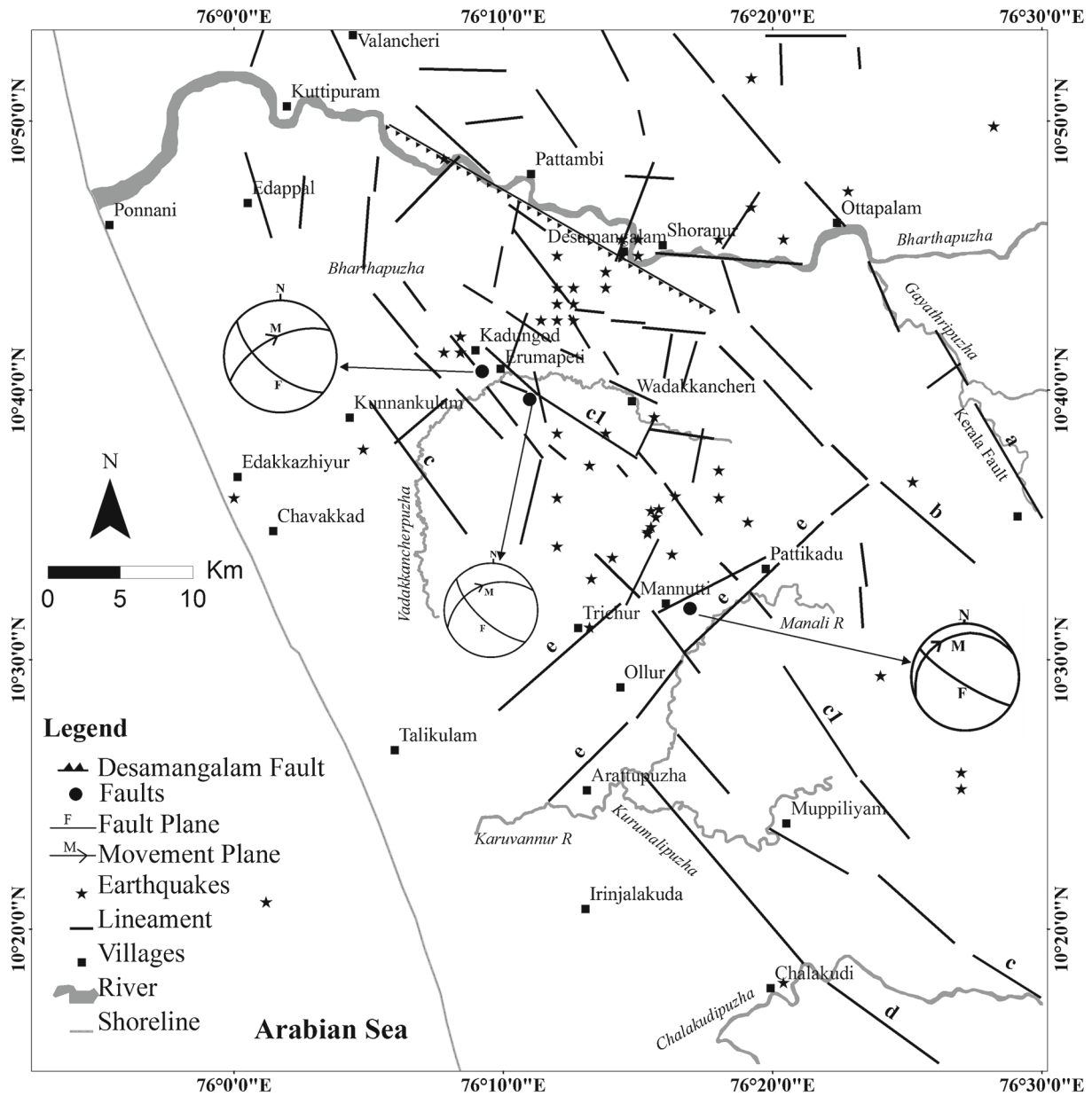


Figure 8. Location of the identified brittle faults and earthquakes within the study area. Movement planes of three faults are plotted to show fault plane and movement plane using the procedure suggested by Marshak and Mitra (1988). Note the spatial association of brittle faults and earthquakes with lineaments.

with the help of single seismological observatory located at Peechi. Though the location accuracy may not be sufficient to confidentially associate them to any particular lineament or to assign a trend, the ongoing seismicity may be the result of the tectonic adjustment along NW–SE structures, which are associated with geomorphic anomalies and faulting (figure 8).

8. Discussion

For better understanding of tectonic processes operating in the area, the study area has been

divided into six zones based on topography and lineament pattern (figure 5). Lineament C1 separates zone I from zone II, and zone IV from zone V. Lineament 'b' separates zone III from zone II and IV. The NE–SW trending Pattikadu lineament (e), running across the study area, separates zones I and II from zones IV and V. The zone VI is demarcated by 'd' lineament separating it from zone V. Each morphometric parameter is statistically analyzed for different zones (figure 6).

The zones I, III and VI lie in low relief area, whereas zones II, IV and V lie in high relief area (figure 6). The study indicates that drainage density (DD) and ruggedness number (R_n) are consistent

with the basin relief (figures 5 and 6) whereas elongation ratio (R_e) do not have much influence on relief. Higher values of bifurcation ratio (R_b) are observed in the NE part of zone I in the vicinity of NW–SE trending lineament ‘c1’, in NE and SE parts of zone II and in the vicinity of NW–SE trending lineament ‘b’ (southeastern continuity of Desamangalam Fault). Higher values of ‘ R_b ’ are also observed at SW part of zone III in the vicinity of NW–SE trending lineament b and in the central part of zone IV. The R_b values are relatively high even though DD is low in zone I (figure 6), which may be an indication of uplift of the block (zone I).

The basins in the area are mostly elongated in shape; however, less elongated basins are also observed in this area randomly. The lineament ‘c1’ across which the Vadakkancheripuzha River changes its course shows anomalously high elongated basin in the southwestern end of the area (figure 5). Similarly, the lineament ‘d’ which may be the reason for compressed meandering of the Kurumalipuzha River is also associated with a very elongated basin (figure 5).

The courses of rivers in the area are also controlled by the NW–SE trending lineaments. The lineament ‘c’ induces a sharp turn towards SE that affected all the rivers (Kurumalipuzha, Manali and Vadakkancheripuzha). The lineament ‘c1’ also influenced the course of the Manali and Vadakkancheripuzha rivers and both of them took SW direction once they cross the lineament. It appears that the meander patterns of smaller rivers are also influenced by the NW–SE trending lineaments and they induced compressed meandering in the upstream, may be due to the change in slope induced by the lineament. Earlier studies identified that compressed meandering is one of the important anomalies that can be attributed to active tectonics (Ramasamy *et al.* 2011). The present observations suggest that the NW–SE trending structural set-up in the area is influencing the drainage network of the area.

The NW–SE trending lineaments that associated with brittle faulting are identified as the continuity of Periyar lineament. At three locations these three faults are developed into visible zones of faulting and damage zones that are dipping SW. Slickensides from these fault zones indicate a consistent north-directed movement of respective hanging wall blocks (figure 8). The sporadic seismicity in the region is also concentrating in this area, which may be an indication of tectonic disturbance. In the southeastern end of Periyar Fault too there were incidences of earthquakes (Rajendran *et al.* 2009).

Peninsular India is suggested to be under compressional stress regime due to the continued northward movement of Indian landmass and the

resistive forces from Himalayan collision zone. In this present scenario, strike slip and reverse faulting are the dominating mechanisms in peninsular India. Studies by Gowd *et al.* (1992) identified that NW–SE trending structural weaknesses are one of the favourable directions that can facilitate movement in the present tectonic regime. The NW–SE trending lineaments and the north directed movements observed in the area may be indicating that these have resulted from the neotectonic movements.

9. Conclusions

The present study delineates three sets of lineaments, viz., NW–SE, NNE–SSW and NE–SW lineaments in the area. The Periyar lineament entering from south into this area appears branched out into three en-echelon segments. The study indicates that the anomalies in morphometric parameters like drainage density (DD), ruggedness number (R_n), bifurcation ratio (R_b) and stream frequency are observed in basins lying around segments of Periyar lineament. Like the Desamangalam Fault (which is identified as active fault), Periyar lineaments seem to exert control on the present drainage system configuration of the area.

The drainage deflections and associated change in meandering pattern are the significant observations for Periyar lineaments. The anomalies in the river sinuosity are mostly confined to these lineaments. A number of brittle faults that appear to be formed in the present tectonic regime are identified to align or parallel the NW–SE trending lineaments, defined by the segments of Periyar lineament. This area is also experiencing frequent seismic activity. The present study suggests that the NW–SE trending Periyar lineaments/faults may be responding to the present regional stress regime and are reflected on subtle adjustment of drainage system.

Acknowledgements

We express our sincere gratitude to the SERB division of the Department of Science and Technology for funding (SR/S4/ES-434/2009) this study. The investigators thank Dr V Venkateswarlu, Director, NIRM for his encouragement, support and facilities. YS, BJ, GPG thank VIT University for permission to publish this work. Director NCESS is thanked for providing earthquake data of the region. We also thank the reviewers for their critical evaluation and helpful suggestions to improve the manuscript.

References

- Basu K L 1964 A note on the Coimbatore earthquake of 8th February 1900; *Indian J. Meteor. Geophys.* **15** 281–286.
- Bhaskar Rao Y J, Chetty T R K, Janardhan A S and Gopalan K 1996 Sm–Nd and Rb–Sr ages and P–T history of the Archaean Sittampundi and Bhavani layered meta-anorthosite complexes in Cauvery shear zone system, south India: Evidence for Neoproterozoic reworking of Archaean crust; *Contrib. Mineral. Petrol.* **125** 237–250.
- Bruhn R L, Parry W T, Yonkee W A and Thomson T 1994 Fracturing and hydrothermal alteration in normal fault zones; *PAGEOPH* **142** 609–644.
- Caine J S, Evans J P and Forster C B 1996 Fault zone architecture and permeability structure; *Geology* **24** 1025–1028.
- Cox R T 1994 Analysis of drainage basin asymmetry as a rapid technique to identify areas of possible Quaternary tilt-block tectonics: An example from the Mississippi embayment; *Geol. Soc. Am. Bull.* **106** 571–581.
- D’Cruz E, Nair P K R and Prasannakumar V 2000 Palghat Gap – a dextral shear zone from the south Indian granulite terrain; *Gondwana Res.* **3** 21–31.
- Drury S A and Holt R W 1980 The tectonic framework of the south Indian craton – a reconnaissance involving LANDSAT imagery; *Tectonophysics*. **65** T1–T15.
- Ghosh J G, de Wit M J and Zartman R E 2004 Age and tectonic evolution of Neoproterozoic ductile shear zones in the southern granulite terrain of India, with implications for Gondwana studies; *Tectonics* **23** 1–38.
- Gowd T N, Srirama Rao S V and Gaur V K 1992 Tectonic stress field in the Indian subcontinent; *J. Geophys. Res.* **97** 11,879–11,888.
- Grady J L 1971 Deep main faults in south India; *J. Geol. Soc. India* **12** 56–62.
- GSI 1992 Quadrangle Geological map; **58B**.
- GSI 2000 *Seismotectonic Atlas of India and its Environs*; GSI Spec. Publ. no. **72**.
- Hare P W and Gardner T W 1985 Geomorphic indicators of vertical neotectonism along converging plate margins, Nicoya Peninsula, Costa Rica; In: *Tectonic Geomorphology* (eds) Morisawa M and Hack J T (Boston: Allen and Unwin), pp. 75–104.
- Holbrook J and Schumm S A 1999 Geomorphic and sedimentary response of the river to tectonic deformation: A brief review and critique of a tool for recognizing subtle epigenetic deformation in modern and ancient setting; *Tectonophysics*. **305** 287–306.
- Horton R E 1945 Erosional development of streams and their drainage basins: Hydrophysical approach to quantitative morphology; *Geol. Soc. Am. Bull.* **56** 275–370.
- IMD 1995 Report on micro earthquake survey in Trichur district Kerala; 18p.
- John B 2003 Characteristics of near surface crustal deformation associated with shield seismicity: Two examples from peninsular India; Unpublished PhD thesis, Cochin University of Science and Technology.
- John B and Rajendran C P 2005 Constraining the pattern of deformation associated with low-displacement faults in the cratonic regions: An example from the Precambrian province of Kerala, south India; *J. Geol. Soc. India* **66** 29–41.
- John B and Rajendran C P 2008 Geomorphic indicators of Neotectonism from the Precambrian terrain of peninsular India: A study from the Bharathapuzha Basin, Kerala; *J. Geol. Soc. India* **71** 827–840.
- John B and Rajendran C P 2009 Evidence of episodic brittle faulting in the cratonic part of the peninsular India and its implications for seismic hazard in slow deforming regions; *Tectonophysics*. **471** 240–252.
- Jorgensen D W 1990 Adjustment of alluvial river morphology and process to localized active tectonics; PhD thesis, Colorado State University, Fort Collins, CO, USA.
- Keller E A and Pinter N 1996 *Active Tectonics*; Prentice Hall International (UK) Ltd., London.
- Krishnaswami V S 1981 The Deccan volcanic episode: Related volcanism and geothermal manifestations; In: Deccan volcanism (eds) Subbarao K V and Sukheswala R N, *Geol. Soc. India Memoir* **3** 1–7.
- Marshak S and Mitra G 1988 *Basic methods of structural geology*; Prentice Hall, 446p.
- Mishra D C, Singh A P and Rao M B S V 1989 Idukki earthquake and the associated tectonics from Gravity study; *J. Geol. Soc. India* **34** 147–151.
- Nair M M 1990 Structural trend line patterns and lineaments of the Western Ghats, south of 13° latitude; *J. Geol. Soc. India* **35** 99–105.
- Ouchi S 1985 Response of alluvial rivers to slow active tectonic movement; *Geol. Soc. Am. Bull.* **96** 504–515.
- Panek T 2004 The use of morphometric parameters in tectonic geomorphology (on the example of western Beskydy Mts); *Geographic* **1** 111–126.
- Rajendran K and Rajendran C P 1995 A report on the December 2, 1994 earthquake; *Technical Report, Centre for Earth Science Studies*, 34p.
- Rajendran C P and Rajendran K 1996 Low-moderate seismicity in the vicinity of Palghat Gap, south India and its implications; *Curr. Sci.* **70** 304–307.
- Rajendran K, Talwani P and Gupta H K 1992 State of stress field in the Indian subcontinent: A review; *Curr. Sci.* **62** 86–93.
- Rajendran C P, John B, Sreekumari K and Rajendran K 2009 Reassessing the earthquake hazard in Kerala based on historical and current seismicity; *J. Geol. Soc. India* **73** 785–802.
- Ramasamy S M, Kumanan C J, Selvakumar R and Saravanavel J 2011 Remote sensing revealed drainage anomalies and related tectonics of south India; *Tectonophysics*. **501** 41–51.
- Rastogi B K, Chadha R K and Sarma C S P 1995 Investigations of June 7, 1988 earthquake of magnitude 4.5 near Idukki Dam in southern India; *PAGEOPH* **145** 109–122.
- Schumm S A 1956 Evolution of drainage systems and slopes in badlands at Perth Amboy; *Geol. Soc. Am., New Jersey* **67** 597–646.
- Schumm S A 2000 *Active Tectonics and Alluvial Rivers*; Cambridge University Press, Cambridge, UK, 276p.
- Singh H N, Raghavan V and Varma A K 1989 Investigation of Idukki earthquake sequence of 7th–8th June 1988; *J. Geol. Soc. India* **34** 133–146.
- Sinha-Roy S and Mathai T 1979 Development of western continental margin of India and plateau uplift as related to geology and tectonics of Kerala; In: *Workshop on Status, Problems and Programmes in Indian shield*, pp. 235–271.
- Strahler A N 1951 *Physical geography*; John Wiley and Sons, Inc., New York, 733p.
- Strahler A N 1957 Quantitative analysis of watershed geomorphology; *Trans. Am. Geophys. Union* **38** 91–920.
- Strahler A N 1964 Quantitative geomorphology of drainage basins and channel networks; In: *Handbook of Applied*

- Hydrology*, McGraw-Hill Book Cooperation, New York, pp. 4-39-4-76.
- Subrahmaniam P 1976 Geotectonic problems of Idamalayar dam site; In: *Geology and Geomorphology of Kerala, Geol. Surv. India (Abstract)* 34.
- Subrahmanya K R 1996 Active intraplate deformation in south India; *Tectonophys.* **262** 231-241.
- Vittala S, Govindaiah S and Honne G H 2004 Morphometric analysis of sub-watersheds in the Pavagada area of Tumkur district, south India using remote sensing and GIS techniques; *J. Indian Soc. Remote Sensing* **32** 351-362.
- Zámolyi A, Székely B, Draganits E and Timár G 2010 Neotectonic control on river sinuosity at the western margin of the Little Hungarian Plain; *Geomorph.*, doi: [10.1016/j.geomorph.2009.06.028](https://doi.org/10.1016/j.geomorph.2009.06.028).
- Zuchiewicz W 1989 Morphotectonic phenomena in the polish flysch Carpathians: A case study of the eastern Beskid-Niski Mountains; *Questiones Geographicae Spec. Issue* **2** 155-167.

MS received 15 September 2015; revised 11 January 2016; accepted 24 January 2016

Corresponding editor: N V CHALAPATHI RAO